Pure Appl. Chem., Vol. 78, No. 8, pp. 1595–1609, 2006.
doi:10.1351/pac200678081595

Solvent conformation and ion solvation: From molecular to ionic liquids*

Shin-ichi Ishiguro‡, Yasuhiro Umebayashi, Kenta Fujii, and Ryo Kanzaki

Department of Chemistry, Faculty of Science, Kyushu University, Hakozaki, Higashi-ku, Fukuoka 812-8581, Japan

Abstract: Metal ions are solvated in solution, and, in a sterically congested organic solvent, those solvent molecules that are simultaneously bound to the metal ion will be subject to consequential steric interactions through space. The molecular structure of a solvent, particularly that of any functional groups in the vicinity of the coordinating atom to the metal ion, plays a key role in the solvation steric effect. Weak solvation steric effects lead to a distorted octahedral structure for six-coordinate transition-metal(II) ions, whereas strong steric effects lead to a decreased solvation number. In particular cases, the conformation of a solvent may undergo a change in response to coordination to the metal ion. Solvation steric effects play a decisive role in reaction thermodynamics and kinetics of the metal ion. Here, we show our recent results on solvation steric effects in terms of structure and thermodynamics, particularly, the conformational change of solvent and its effect on the metal-ion complexation.

Keywords: solution chemistry; solvent conformation; solvation structure; conformational change; molecular liquids; ionic liquids.

INTRODUCTION

Molecular liquids, not only water but also a variety of organic compounds, have been widely used as solvents [1], and recently, room temperature ionic liquids (RTILs) receive increasing attention as new media for organic reactions and solvent extractions, as well as noble electrolyte materials [2–13]. Solute molecules and ions are strongly solvated in solution to form solvation clusters, and thus their reactions and properties in solution depend on the solvent [14–17]. Here, specific and unusual aspects are seen in the structures and reactions when steric effects play a significant role in solute–solvent and solvent–solvent interactions. This has indeed been demonstrated in various systems and phenomena involving solvolytic reactions [18–23], solvation dynamics [24], reaction kinetics and rates [25–28], and spectroscopic properties [29–31]. Steric solvent effects upon solvation to the metal ion are also seen in the lithiation selectivity for amines [32], aggregation of lithium thioamidates [33], and redox potentials [34,35]. The roles of steric and electrostatic factors in determining the orientation and dynamic behavior have been studied for benzimidazole-type ligands in Ru^{II}(dimethyl sulfoxide) complexes [36]. Theoretical approaches to steric effects have also been reported on the hydrogen-bonding intermolecular structure [37], conformational change [38], ion solvation [39], protonation [40], and reaction mechanisms [41–43].

*Paper based on a presentation at the 29th International Conference on Solution Chemistry, Portorož, Slovenia, 20–25 August 2005. Other presentations are published in this issue, pp. 1559–1617.

‡Corresponding author

It is well known that the conformation of a molecule profoundly influences its reactivity and intermolecular interactions. 2,2'-Bipyridine, for instance, changes its conformation from the *trans* to *cis* form upon complexation to the metal ion [44]. Diethylenetriamine (dien) is protonated to yield two conformers of $Hdien^+$, the linear and folded ones, in an aqueous solution [45]. A similar situation also applies for particular solvents, in which two conformers coexist in equilibrium in the liquid state, and the conformation varies upon solvation to the metal ion. Here, we briefly summarize our recent works on the conformation of solvent, in both molecular and ionic liquids. Conformational change of solvent upon solvation to the metal ion or complexes will also be described in terms of the solvation steric effect.

SOLVATION STERIC EFFECT

Ion solvation is essential and indispensable for metal salts to be dissolved in a solvent. The solvation number, or the number of solvent molecules simultaneously bound to a metal ion, has been determined in water as well as organic solvents [46]. The nickel(II) ion is six-coordinated in dimethyl sulfoxide and *N,N*-dimethylformamide (DMF), as well as water, and the geometry of the solvate ion is a regular octahedron, indicating that practically no appreciable solvation steric effect, or solvent–solvent interaction through space, operates among solvent molecules simultaneously bound to the metal ion. The nickel(II) ion is also six-coordinated in *N,N*-dimethylacetamide (DMA) and *N*-methylpropionamide (NMP), whereas the solution color of nickel(II) perchlorate is yellow, unlike green in DMF, implying that an octahedral coordination structure is distorted. Solution color is red, i.e., the nickel(II) ion is five-coordinated, in *N,N*-dimethylpropionamide (DMPA) and *N*,*N*,*N*',*N*'-tetramethylurea (TMU). The coordination geometry of the solvate ion is distorted, or the solvation number even reduces in some solvents. Solvents such as DMA, NMA, DMPA, and TMU involve bulky functional groups, implying that the local steric congestion of solvent, particularly in the vicinity of the coordinating atom to the metal ion, plays a key role in the solvation steric effect.

The solvation steric effect leads to an enhanced metal-ion complexation. In Fig. 1, as an example, species distributions in the manganese(II) bromide system in DMF, DMA, NMP, DMPA, and TMU are compared [47–49]. As seen, the complexation is enhanced in DMA and NMP almost to the same extent over DMF, and is markedly enhanced in DMPA and TMU. This enhancement is mainly ascribed to the enthalpy term, i.e., the metal–solvent interaction may be weakened when the coordination sphere is sterically congested.

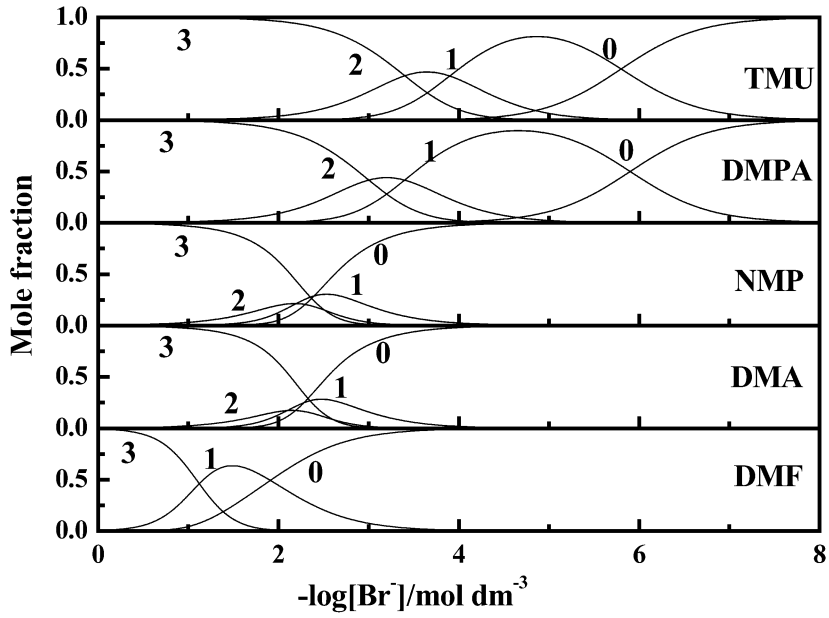

Fig. 1 Species distributions in the Mn^{2+}–Br^- system at 298 K.

CONFORMATIONAL EQUILIBRIUM OF SOLVENT IN THE BULK

The nature of solvents is related to their liquid structures, and thus chemists have devoted a lot of effort to reveal solvent structure, or the structure of molecular aggregates (clusters), in the liquid state. Various types of hydrogen-bonded clusters are formed among solvent molecules in protic solvents, as well as water. Aprotic solvents also form clusters in the liquid state, although their interactions are generally weak [50]. Structures of solvent clusters and their distribution depend on temperature and pressure, and also on the composition of solvent mixtures [51]. A kind of solvent involves structural isomers that are present in equilibrium in the liquid state. A typical example is DMPA, $CH_3CH_2(CO)N(CH_3)_2$, in which the propionyl group can rotate along the single CH_3–CH_2 bond to yield conformers [52]. Indeed, an observed Raman spectrum of neat DMPA in Fig. 2 shows bands at 711 and 760 cm^{-1}, both of which are assigned to the symmetric stretching N–CH_3 vibration. The two bands cannot be reproduced by theoretical calculations for a given conformer of DMPA. Scheme 1 shows the geometries of the planar *cis*, nonplanar staggered, and planar *trans* conformers, where the terminal methyl group of the planar *cis* and *trans* conformers locates inside the amide O–C–N plane, and that of the nonplanar staggered conformer locates upside. The self-consistent field (SCF) energies of these conformers were evaluated by theoretical molecular orbital (MO) calculations. The torsion energy profile thus obtained by varying propionyl C–C–C–O dihedral angle is shown in Fig. 3 (the solid line), indicating that the planar *cis* conformer has the lowest energy and a local minimum appears at angle about 90° (the nonplanar staggered conformer). According to our MO calculations followed by normal coordinate analyses for the conformers, the bands at 711 and 760 cm^{-1} are ascribed to the nonplanar staggered and planar *cis* conformers, respectively, indicating that two conformers are present in equilibrium in neat solvent. By analyzing intensities of these Raman bands at varying temperature, the equilibrium constant, enthalpy, and entropy of conformational change are determined. The enthalpy value of 5.0 kJ mol^{-1} was indeed obtained for the conformational change from the planar *cis* to nonplanar staggered form, the value being in good agreement with that predicted by theoretical calculations.

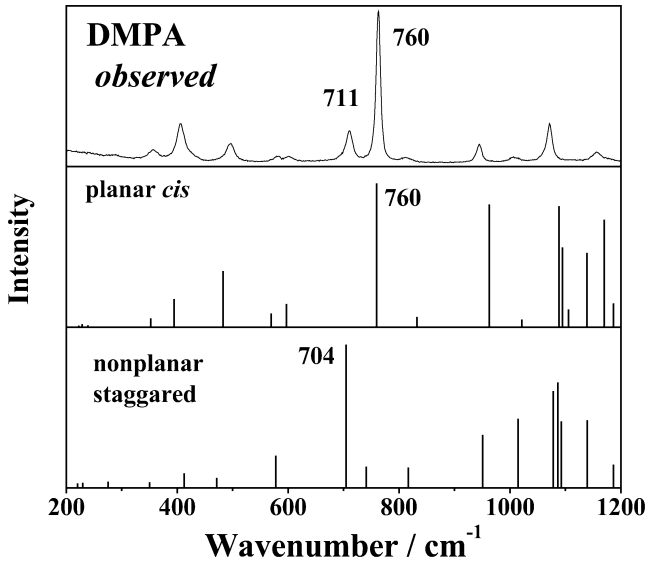

Fig. 2 An observed Raman spectrum of neat DMPA at 298 K, and vibrational frequencies of the planar *cis* and nonplanar staggered conformers of DMPA predicted by ab initio MO calculation followed by normal coordinate analyses using the B3LYP6-31G(d) basis set.

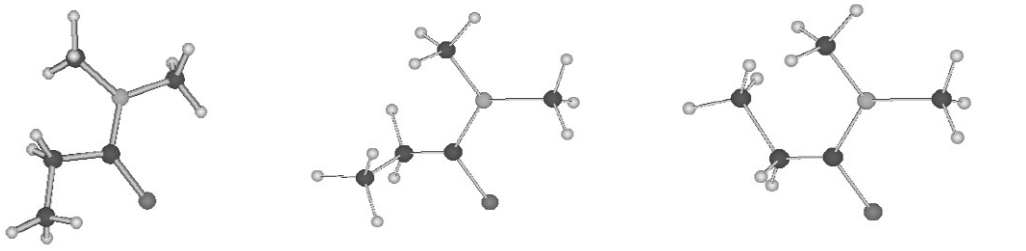

Scheme 1 Geometries of DMPA conformers.

The torsion energy profile for the protonated DMPA is also shown in Fig. 3 (the broken line). No significant difference in the potential energy surface is found between the protonated and nonprotonated DMPA. This indicates that, unlike dien [45], the intramolecular charge distribution of DMPA is hardly changed by protonation. The same applies also for the metal solvates, in which the metal ion binds one or two DMPA molecules [53]. The torsion energy profile of DMPA within the $Zn(DMPA)_2^{2+}$ solvate ion in Fig. 4 is indeed similar to that of the isolated DMPA, evidently indicating that the intramolecular charge distribution of DMPA bound to the metal ion remains practically unchanged, if no steric hindrance operates among solvent molecules simultaneously bound to the metal ion.

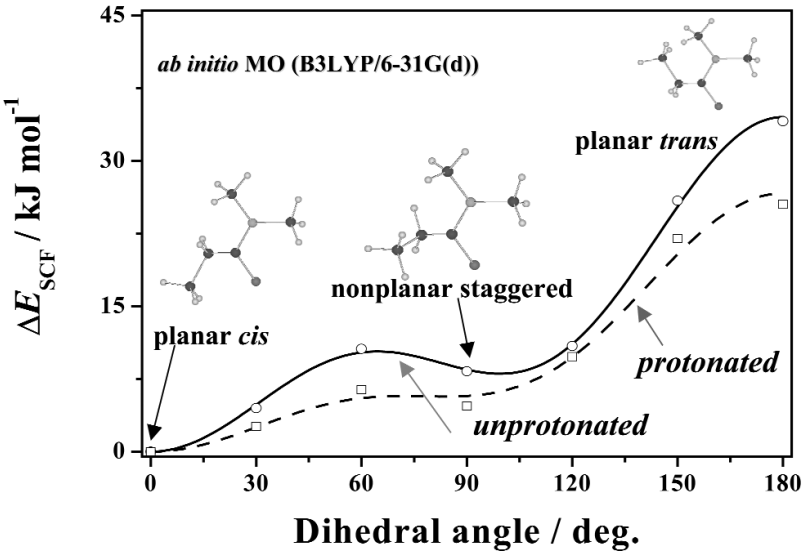

Fig. 3 Torsion energy profiles of protonated and unprotonated DMPA as a function of the propionyl C–C–C–O dihedral angle.

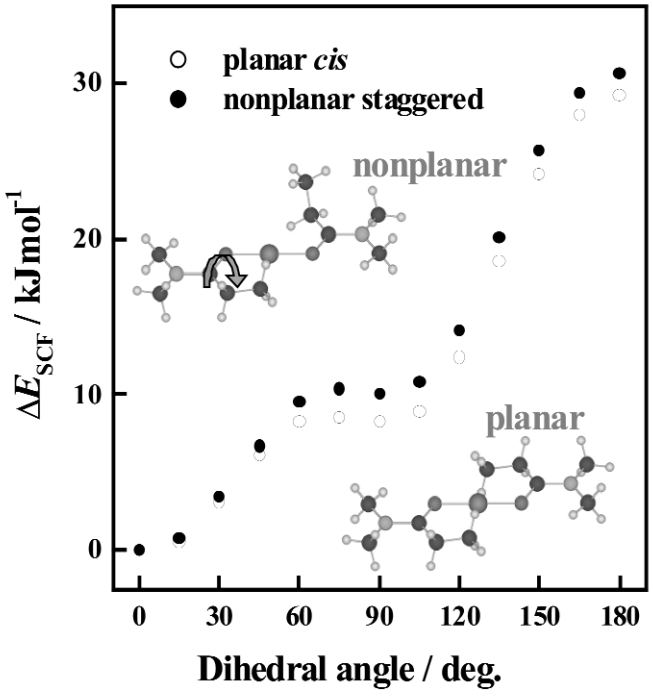

Fig. 4 Torsion energy profiles of DMPA within the $[Zn(DMPA)(planar\ cis\text{-}DMPA)]^{2+}$ and $[Zn(DMPA)(nonplanar\ staggered\ DMPA)]^{2+}$ as a function of the propionyl C–C–C–O dihedral angle.

Dimethylcarbonate (DMC) is used as a component of solvent mixtures for batteries, together with such solvents as ethylene carbonate (EC) and propylene carbonate (PC). The dielectric constant of DMC is 0.87 D, which is significantly smaller than that of EC (4.87 D) and PC (0.94 D), whereas the

electron-pair donating and accepting properties are similar (e.g., the Gutmann's donor number [54,55] is 17.2, 16.4, and 15.1 and the E_{T30} value [12,55] is 38.2, 48.6, and 46.0 for DMC, EC, and PC, respectively). DMC yields two planar conformers, *cis–cis* and *cis–trans*, with respect to the carbonyl O-atom (Scheme 2), both of which are stable relative to the nonplanar conformers. The SCF energy profile shows that the *cis–cis* conformer is more favorable by ca. 8 kJ mol^{-1} than the *cis–trans* one, indicating that the *cis–cis* conformer is the main species in the bulk solvent at room temperature. Indeed, DMC shows strong Raman bands, and their frequencies are well reproduced by MO calculations followed by normal coordinate analyses for the optimized geometry of the *cis–cis* conformer [56]. However, DMC shows also weak Raman bands that cannot be ascribed to the *cis–cis* conformer, indicating that the *cis–trans* conformer is also present in equilibrium in the bulk, although it is a minor species. Indeed, frequencies of the observed weak Raman bands are reproduced by theoretical calculations for the *cis–trans* conformer.

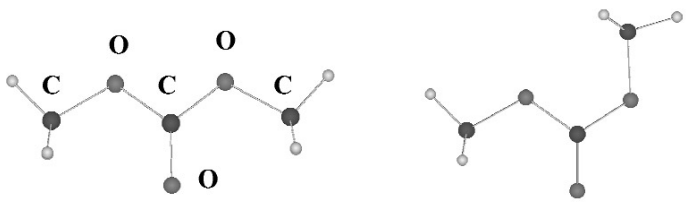

Scheme 2 Geometries of DMC conformers.

Imidazolium (EMI^+) salts are known as typical RTILs. The EMI^+ cation in Scheme 3 contains an ethyl group linked to the N1 atom of the imidazolium ring, which can rotate to yield conformers. As seen in Fig. 5, the nonplanar staggered conformer is more favorable than the planar one, although the energy gap is very small. The two conformers of EMI^+ are present in equilibrium in RTILs of its BF_4^-, PF_6^-, $CF_3SO_3^-$, and bis(trifuloromethanesulfonyl) imide ($TFSI^- = N(CF_3SO_2)_2^-$) salts [57]. The enthalpy of conformational change experimentally obtained by analyzing Raman band intensities of the conformers at varying temperature is practically the same as that evaluated by theoretical calculations.

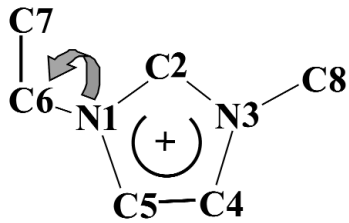

Scheme 3 The skeleton of the EMI^+ cation.

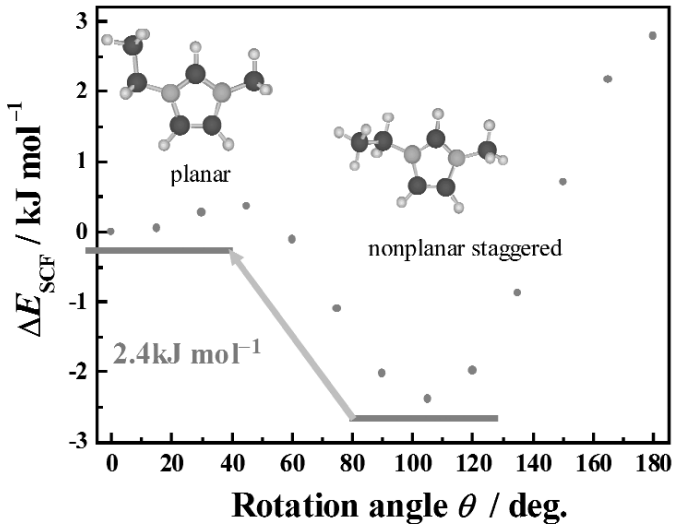

Fig. 5 Torsion energy profile of EMI^+ as a function of the C–C–N–C dihedral angle.

Raman spectra of EMI^+TFSI^- show relatively strong bands arising from $TFSI^-$ at about 398 and 407 cm^{-1}. The 407 cm^{-1} band, relative to the 398 cm^{-1} one, is appreciably intensified with raising temperature, suggesting that conformational equilibrium is established for $TFSI^-$ in the liquid state. According to density functional theory (DFT) calculations followed by normal frequency analyses, two conformers of the C_2 and C_1 symmetries gave global and local minima, respectively, with an energy difference 2.2–3.3 kJ mol^{-1}, and the wagging ω-SO_2 vibration of $TFSI^-$ appears over the range 380–440 cm^{-1}. The enthalpy of conformational change from C_2 to C_1 was evaluated by analyzing Raman band intensities of the conformers at varying temperature. The enthalpy value is in good agreement with that obtained by theoretical calculations [58].

STERICALLY INDUCED CONFORMATIONAL CHANGE OF SOLVENT UPON SOLVATION [52,59]

The metal ion is solvated in solution. In zinc(II) perchlorate DMPA solutions, solvent molecules bound to the metal ion show Raman bands at higher frequencies than those of free solvent molecules in the bulk, Fig. 6. As seen, with increasing molality of the metal ion, the intensity I_b of the bound DMPA increases and the intensity I_f of the free DMPA decreases. The solvation number n and the Raman scattering coefficient J can then be evaluated by plotting I_f against the molality of the metal ion. In the case of Zn^{2+}, it revealed that the metal ion is four-coordinated in DMPA. Here, note that the intensity of the bound nonplanar staggered conformer is significantly larger than that of the bound planar *cis* one. This implies that the nonplanar staggered conformer is more favorable than the planar *cis* one in the coordination sphere, i.e., the conformation of DMPA changes from the planar *cis* to nonplanar staggered form upon solvation to the metal ion. Indeed, the enthalpy value of conformational change from the planar *cis* to nonplanar staggered form, evaluated by analyzing Raman spectra measured at varying temperature, is negative, unlike the value of free DMPA in the bulk, indicating that the nonplanar staggered conformer is more preferable in the coordination sphere of the metal ion. As seen in Fig. 7, the enthalpy value depends on the metal ion, i.e., the value increases with increasing ionic radius for alkaline earth metal ions, Mg^{2+}, Ca^{2+}, and Sr^{2+}, indicating that the steric congestion in the coordination sphere increases with decreasing ionic radius of the metal ion. With transition-metal(II) ions, the values are all more negative and large.

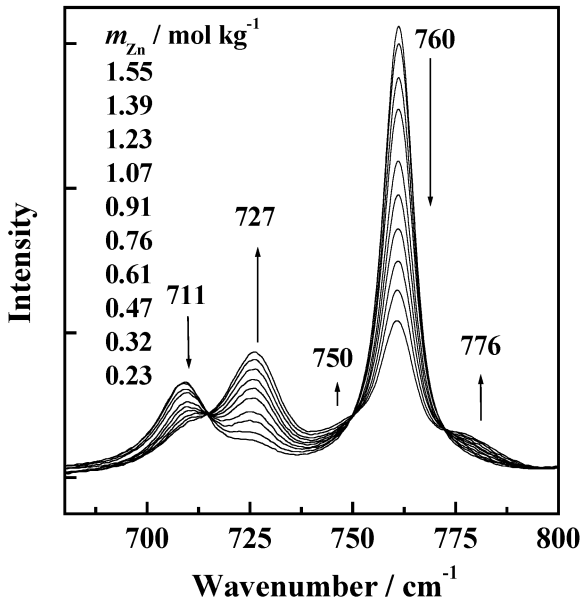

Fig. 6 Raman spectra of $Zn(ClO_4)_2$ DMPA solutions at varying molality at 298 K.

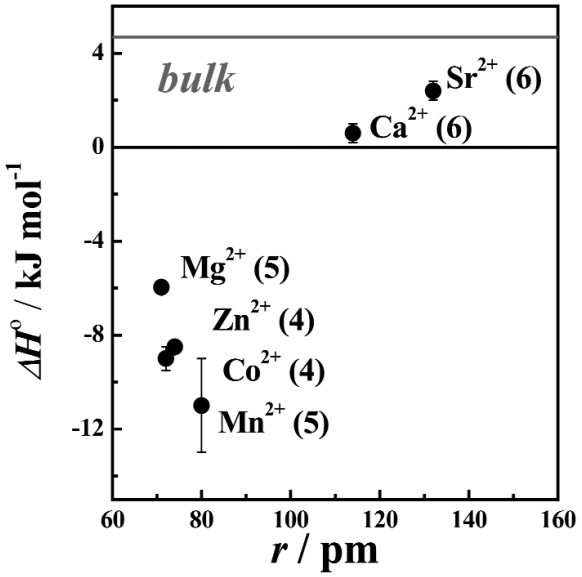

Fig. 7 Enthalpies of conformational change of DMPA bound to metal ions.

As the zinc(II) ion is four-solvated in DMPA, we calculated relative energies of the tetra-solvate zinc(II) ion [Zn(planar *cis*-DMPA)$_{4-n}$(nonplanar staggered-DMPA)$_n$]$^{2+}$ (n = 0–4) [58]. As seen in Fig. 8, the relative SCF energy decreases with stepwise replacement of the planar *cis*-DMPA with the nonplanar staggered-DMPA. Note that, as described in a previous section, the planar *cis* conformer is preferred in the coordination sphere of the di-solvate complex, in which there is no steric interaction between bound solvent molecules. The SCF energy decreases with increasing n in the tetra-solvate

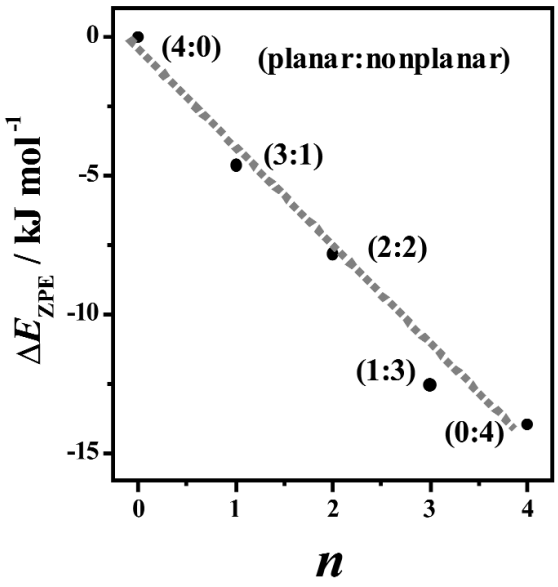

Fig. 8 SCF energies of [Zn(planar *cis*-DMPA)$_{4-n}$(nonplanar staggered-DMPA)$_n$]$^{2+}$ (n = 0–4) complexes (4-n:n).

zinc(II) ion, which indicates that four-coordination of the planar *cis*-DMPA conformer is sterically hindered, and a part of planar *cis* conformers changes their conformation to reduce steric congestion.

EFFECT OF CONFORMATIONAL CHANGE ON THE METAL-ION COMPLEXATION [60]

TMU has a similar molecular geometry to that of the planar *cis*-DMPA, if we take into account their local geometries in the vicinity of the carbonyl O-atom, and thus TMU is considered to be an analog of the planar *cis*-DMPA. Calorimetric titration curves for the bromo complexation of the manganese(II) ion in TMU and DMPA are compared in Fig. 9. As seen, the formation enthalpy of $MnBr^+$ is positive in DMPA, whereas it is negative in TMU, despite the fact that the metal ion is five-solvated in both the solvents. This implies that the solvation enthalpy of the manganese(II) ion in TMU is smaller than that in DMPA (note that the solvation enthalpy of the Br^- ion is not appreciably different in these solvents). This is unexpected because the electron-pair donating ability of TMU is stronger than that of DMPA [55].

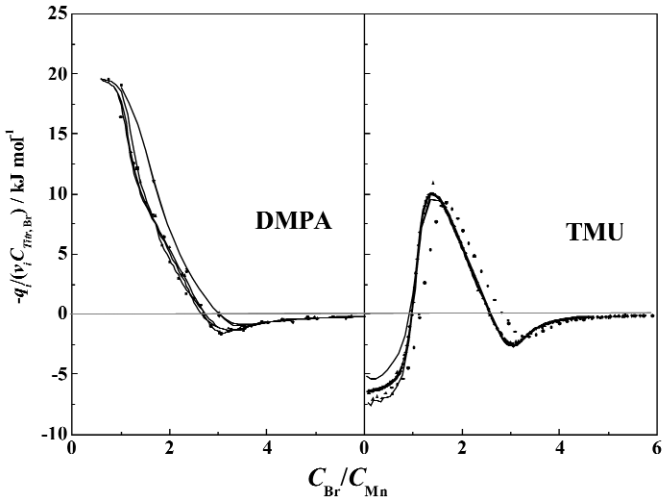

Fig. 9 Calorimetric titration curves in the Mn^{2+}–Br^- system in DMPA and TMU containing 0.1 mol dm^{-3} $(C_2H_5)_4NClO_4$ as an ionic medium at 298 K.

The difference formation enthalpy of $MnBr^+$ in DMPA and TMU is represented in more detail in terms of enthalpies of transfer of related species on the basis of a thermodynamic cycle as follows:

$$\Delta H_1^\circ(\mathrm{TMU}) - \Delta H_1^\circ(\mathrm{DMPA}) = \Delta_t H^\circ(\mathrm{MnBr^+}) - \Delta_t H^\circ(\mathrm{Mn^{2+}}) - \Delta_t H^\circ(\mathrm{Br^-}) \quad (1)$$

where ΔH_1°(solvent) denotes the formation enthalpy of $MnBr^+$ in a solvent, and $\Delta_t H^\circ(i)$ the enthalpy of transfer of species i from DMPA to TMU. The values of $\Delta_t H^\circ(Mn^{2+})$ and $\Delta_t H^\circ(Br^-)$ have been determined to be 25.5 and 0.2 kJ mol^{-1}, respectively, by measuring heats of solution of various salt crystals in these solvents, and by dividing the values into contributions of each ionic component on the basis of the extra-thermodynamic tetraphenylarsonium-tetraphenylborate assumption. The $\Delta_t H^\circ(MnBr^+)$ value is then calculated according to eq. 1 by knowing the $\Delta_t H^\circ(Mn^{2+})$ and $\Delta_t H^\circ(Br^-)$ values. The $\Delta_t H^\circ$ values of $MnBr_2$ and $MnBr_3^-$ are also calculated according to the corresponding equations for ΔH_2° and ΔH_3°, respectively. The $\Delta_t H^\circ$ values for $MnBr_n^{(2-n)+}$ (n = 0–3) are shown in Fig. 10. As seen, the $\Delta_t H^\circ$ values are all negative and small, except for the $\Delta_t H^\circ(Mn^{2+})$. The negative and small $\Delta_t H^\circ$ values are expected, if we take into account a larger electron-pair donating ability of TMU than that of DMPA. The $\Delta_t H^\circ(Mn^{2+})$ value is positive and significantly large, i.e., the solvation energy of the metal ion in TMU is less than that in DMPA, which cannot simply be explained in terms of the electron-pair donating ability of solvent. The metal ion is five-coordinated in both TMU and DMPA, and here, the conformational change of DMPA plays an essential role in the thermodynamic behavior as follows. As described in a previous section, the planar *cis*-DMPA suffers from a stronger steric hindrance than the nonplanar staggered-DMPA in the coordination sphere of the five-coordinated solvate ion. DMPA thus changes its conformation from the planar *cis* to nonplanar staggered form within the $Mn(DMPA)_5^{2+}$ to reduce the steric congestion in the coordination sphere. In contrast, TMU molecules, an analog of the planar *cis*-DMPA, hardly change its conformation, even if they suffer from a strong steric hindrance in the $Mn(TMU)_5^{2+}$.

The enthalpy value of 11 kJ mol^{-1} has been obtained for the conformational change from the planar *cis* to nonplanar staggered form for DMPA bound to the manganese(II) ion. If we take into account that the molecular conformation changes for DMPA but not for TMU, and that an energy of the metal–solvent bond is almost to the same extent for both the solvents, the enthalpy of transfer of Mn^{2+} from DMPA to TMU may be equivalent to the energy of conformational change from the nonplanar staggered conformer to the planar *cis* one. The value $\Delta_t H^\circ(Mn^{2+})$ = 25.5 kJ mol^{-1} from DMPA to TMU

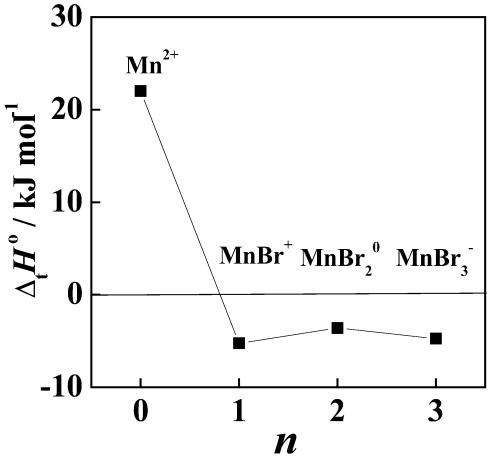

Fig. 10 Enthalpies of transfer of $MnBr_n^{(2-n)+}$ (n = 0–3) from DMPA to TMU at 298 K.

implies that two or three DMPA molecules change their conformation from the planar *cis* to nonplanar staggered form.

The enthalpies of transfer of $MnBr_n^{(2-n)+}$ from DMPA to TMU are all negative and small, implying that the solvation steric hindrance is weak. This means that the nonplanar staggered conformer occurring in the $Mn(DMPA)_5^{2+}$ changes to the planar *cis* one upon complexation to form $MnBr(DMPA)_4^+$, which lead to a different thermodynamic aspect of complexation in DMPA compared to TMU.

CONFORMATION OF SOLVATED METAL ION IN CRYSTALS

As described in a previous section, TMU is an analog of the planar *cis*-DMPA. Similarly, NMP is an analog of the planar *trans*-DMPA, if we take into account the local geometry in the vicinity of the carbonyl O-atom, Scheme 4. If the same solvation number is taken into account, the extent of steric congestion in the coordination sphere of the metal DMPA solvates may be weak in the order of the conformers, planar *cis* > nonplanar staggered > planar *trans*. This implies that the solvation steric hindrance in the coordination sphere of a given metal ion is relatively strong for the TMU (an analog of the planar *cis*-DMPA) solvate, medium for the nonplanar staggered DMPA solvate and weak for the NMP (an analog of the planar *trans*-DMPA) solvate. The solvation number of a given metal ion must thus increase with decreasing solvation steric hindrance. Indeed, as seen in Fig. 11, the solvation number of the cobalt(II) ion is four, five, and six in TMU, DMPA, and NMP solvate crystals, respectively [61].

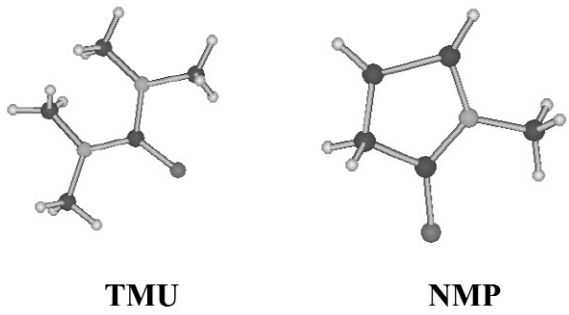

Scheme 4 Geometries of TMU and NMP.

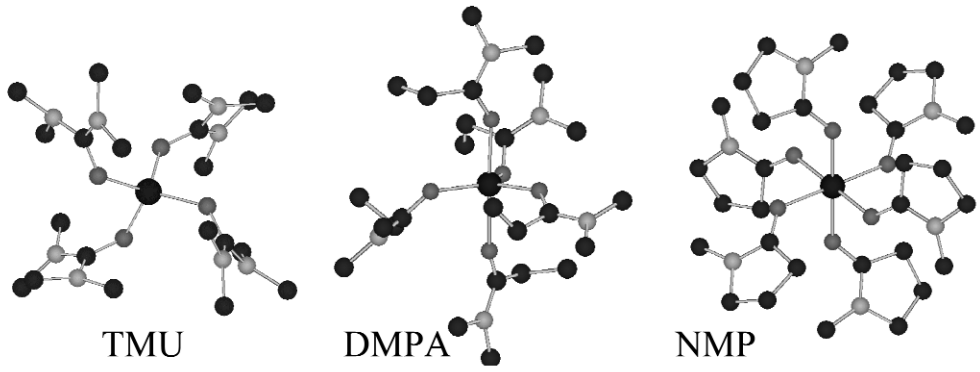

Fig. 11 Crystal structures of $Co(TMU)_4^{2+}$, $Co(DMPA)_5^{2+}$, and $Co(NMP)_6^{2+}$ in their perchlorate salts.

Here, note that all DMPA molecules solvated to the cobalt(II) ion in crystals have the nonplanar staggered form. Figure 12 demonstrates that the nickel(II) and zinc(II) ions are six- and five-solvated, respectively, in their DMPA solvate crystals and all DMPA molecules have the nonplanar staggered form, as well. The copper(II) ion yields two DMPA solvate crystals **1** and **2** of five-coordination. All DMPA molecules in crystal **1** have the nonplanar staggered form, whereas one of five DMPA molecules in crystal **2** has the planar *cis* form. The former crystal is more stable than the latter. In solution, as described in a previous section, the metal DMPA solvate ions involve both planar *cis* and nonplanar staggered conformers. Also, note that the solvation number in these DMPA solvate crystals is larger by one than that in the solution, i.e., the steric congestion in the coordination sphere of the solvate metal ion in crystals is stronger than that in solution, which may lead to a complete conformational change from the planar *cis* to nonplanar staggered form in the solvate crystals.

According to DSC (differential scanning calorimetry) measurements of a series of DMPA solvates of transition-metal(II) ions, the freezing point of all the solvates except for $Ni(DMPA)_6(ClO_4)_2$ (34 °C) is lower than 25 °C, indicating that these solvates are unusually in the liquid state at room temperature. Consequently, these salts may be classified into a kind of RTILs. The reason why the freezing point of these electrolytes is significantly lower than that of the corresponding electrolytes of other solvents is still not established. We suppose at the present stage that, like other RTILs, the conformational freedom of the bound DMPA molecules seems to play an essential role in lowering the melting point.

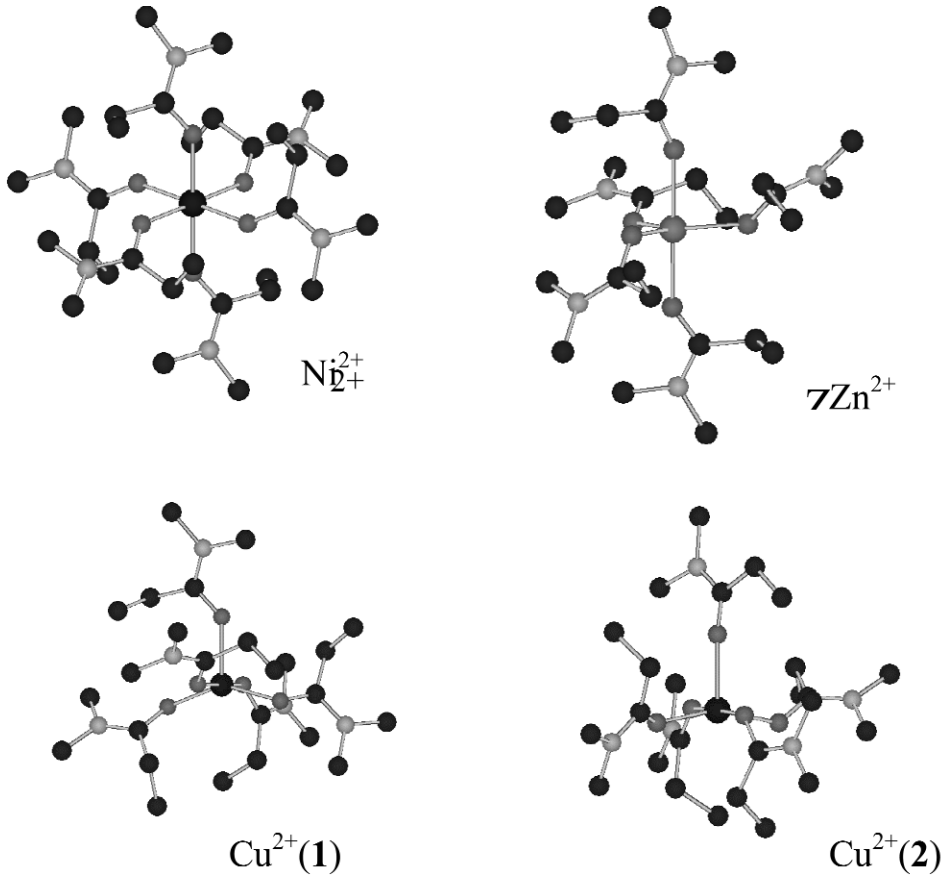

Fig. 12 Crystal structures of $Ni(DMPA)_6^{2+}$, $Cu(DMPA)_5^{2+}$, and $Zn(DMPA)_5^{2+}$ in their perchlorate salts.

ACKNOWLEDGMENTS

This work has been financially supported by Grant-in-Aids for Scientific Research 13440222 and 15750052 from the Ministry of Education, Culture, Sports, Science and Technology of Japan, and also by Grant for Basic Science Research Project from the Sumitomo Foundation.

REFERENCES

1. J. A. Riddick, W. B. Bunger, T. K. Sakano. *Organic Solvents IV*, Wiley-Interscience, New York (1986).
2. R. D. Rogers, K. R. Seddon. *Ionic Liquids as Green Solvents, Progress and Properties*, ACS Symposium Series 856, Oxford University Press, Washington, DC (2003).
3. D. J. Adams, P. J. Dyson, S. J. Tavener. *Chemistry in Alternative Reaction Media*, John Wiley, West Sussex, UK (2004).
4. P. K. Mandall, S. Saha, R. Karmakarl, A. Samantal. *Curr. Sci.* **90**, 301 (2006).
5. S. Pandey. *Anal. Chim. Acta* **556**, 38 (2006).
6. K. R. Harris, L. A. Woolf. *J. Chem. Eng. Data* **50**, 1777 (2005).
7. M. Koel. *Crit. Rev. Anal. Chem.* **35**, 177 (2005).
8. J. Ding, D. W. Armstrong. *Chirality* **17**, 281 (2005).
9. C. Chiappe, D. Pieraccini. *J. Phys. Org. Chem.* **18**, 275 (2005).

10. M. C. Buzzeo, R. G. Evans, R. G. Compton. *ChemPhysChem* **5**, 1106 (2004).
11. C. F. Poole. *J. Chromatogr., A* **49**, 1037 (2004).
12. J. Dupont. *J. Braz. Chem. Soc.* **15**, 341 (2004).
13. F. van Rantwijk, R. M. Lau, R. A. Sheldon. *Trends Biotechnol.* **21**, 131 (2003).
14. C. Reichardt. *Solvents and Solvent Effects in Organic Chemistry*, VCH, Weinheim (1988).
15. A. R. Katritzky, D. C. Fara, H. Yang, K. Tämm. *Chem. Rev.* **104**, 175 (2004).
16. M. Dirand, M. Bouroukba, V. Chevallier, D. Petitjean. *J. Chem. Eng. Data* **47**, 115 (2002).
17. J. Luettmer-Strathmann, J. A. Schoenhard, J. E. G. Lipson. *Macromolecules* **31**, 9231 (1998).
18. S. F. Yunes, J. C. Gesser, H. Chaimovich, F. Nome. *J. Phys. Org. Chem.* **10**, 461 (1997).
19. T. W. Bentley, G. Llewellyn, Z. H. Ryul. *J. Org. Chem.* **63**, 4654 (1998).
20. K. Takeuchi, M. Takasuka, E. Shiba, T. Kinoshita, T. Okazaki, J. M. Abboud, R. Notario, O. Castaño. *J. Am. Chem. Soc.* **122**, 7351 (2000).
21. K. Takeuchi, T. Okazaki, T. Kitagawa, T. Ushino, K. Ueda, T. Endo. *J. Org. Chem.* **66**, 2034 (2001).
22. J. J. Gajewski. *J. Am. Chem. Soc.* **123**, 10877 (2001).
23. N. E. Ponomarev, K. V. Michkov, G. F. Dvorko. *Russ. J. General Chem.* **71**, 591 (2001).
24. N. H. Damrauer, J. K. McCusker. *Inorg. Chem.* **38**, 4268 (1999).
25. C. F. Bernasconi, R. L. Montañez. *J. Org. Chem.* **62**, 8162 (1997).
26. A. Bagno, R. L. Boso, N. Ferrari, G. Scorrano. *Eur. J. Org. Chem.* 1507 (1999).
27. Y. G. Shtyrlin, G. R. Shaikhutdinova, E. N. Klimovitskii. *Russ. J. Gen. Chem.* **71**, 464 (2001).
28. P. Zhao, D. B. Collum. *J. Am. Chem. Soc.* **125**, 14411 (2003).
29. B. Keller, J. Legendziewicz, J. Glinski. *Spectrochim. Acta, Part A* **54**, 2207 (1998).
30. E. B. Tada, L. P. Novaki, O. A. El Seoud. *J. Phys. Org. Chem.* **13**, 679 (2000).
31. C. L. Perrin, J. Kuperman. *J. Am. Chem. Soc.* **125**, 8846 (2003).
32. D. R. Armstrong, A. Carstairs, K. W. Henderson. *Organometallics* **18**, 3589 (1999).
33. T. Chivers, A. Downard, M. Parvez. *Inorg. Chem.* **38**, 5565 (1999).
34. T. Clark, M. Hennemann, R. van Eldik, D. Meyerstein. *Inorg. Chem.* **41**, 2927 (2002).
35. E. A. Ambundo, M. Deydier, A. J. Grall, N. Aguera-Vega, L. T. Dressel, T. H. Cooper, M. J. Heeg, L. A. Ochrymowycz, D. B. Rorabacher. *Inorg. Chem.* **38**, 4233 (1999).
36. E. Alessio, E. Iengo, E. Zangrando, S. Geremia, P. A. Marzilli, M. Calligaris. *Eur. J. Inorg. Chem.* 2207 (2000).
37. H. Adalsteinsson, A. H. Maulitz, T. C. Bruice. *J. Am. Chem. Soc.* **118**, 7689 (1996).
38. B. L. Lucht, M. P. Bernstein, J. F. Remenar, D. B. Collum. *J. Am. Chem. Soc.* **118**, 10707 (1996).
39. R. A. Marcus. *J. Phys. Chem. A* **101**, 4072 (1997).
40. A. A. Mohamed, F. Jensen. *J. Phys. Chem. A* **105**, 3259 (2001).
41. G. Lanza, I. L. Fragalà, T. J. Marks. *J. Am. Chem. Soc.* **122**, 12764 (2000).
42. C. O. da Silva, B. Mennucci, T. Vreven. *J. Phys. Chem. A* **107**, 6630 (2003).
43. J. Roithová, O. Exner. *J. Phys. Org. Chem.* **14**, 752 (2001).
44. M. Komiya, S. Yoshida, S. Ishiguro. *J. Solution Chem.* **29**, 165 (2000).
45. T. Maki, R. Kanzaki, Y. Umebayashi, S. Ishiguro. *Chem. Lett.* **20**, 415 (2004).

46. (a) G. Johansson. *Adv. Inorg. Chem*. **39**, 159 (1992); (b) H. Ohtaki, T. Radnai. *Chem. Rev*. **93**, 1157 (1993); (c) J. L. Fulton, S. D. M. Heald, Y. S. Badyal, J. M. Simoson. *J. Phys. Chem.* **107**, 4688 (2003); (d) K. Ozutsumi, K. Tohji, Y. Udagawa, Y. Abe, S. Ishiguro. *Inorg. Chim. Acta* **191**, 183 (1992); (e) K. Ozutsumi, Y. Abe, R. Takahashi, S. Ishiguro. *J. Phys. Chem.* **98**, 9894 (1994); (f) Y. Inada, K. Sugimoto, K. Ozutsumi, S. Funahashi. *Inorg. Chem*. **33**, 1875 (1994); (g) C. M. V. Stalhandske, I. Persson, M. Sandstrom, M. Alberg. *Inorg. Chem.* **36**, 4945 (1997); (h) Y. Tsutsui, K. Sugimoto, H. Wasada, Y. Inada, S. Funahashi. *J. Phys. Chem.* **101**, 2900 (1997); (i) Y. Inada, H. Hayashi, K. Sugimoto, S. Funahashi. *J. Phys. Chem*. *A* **103**, 1401 (1999); (j) G. Moreau, R. Scopelliti, L. Helm, J. Purans, A. E. Merbach. *J. Phys. Chem. A* **106**, 9612 (2002); (k) O. Kristiansson, I. Persson, D. Bobics, D. W. Xu. *Inorg*. *Chim. Acta* **344**, 15 (2003); (l) K. Ozutsumi, Y. Abe, S. Ishiguro. *J. Phys. Chem*. **98**, 9894 (1994); (m) S. Ishiguro, Y. Umebayashi, R. Kanzaki. *Anal. Sci.* **20**, 415 (2004).
47. S. Ishiguro. *Bull. Chem. Soc. Jpn*. **70**, 1465 (1997).
48. (a) K. Ozutsumi, S. Ishiguro. *J. Chem. Soc., Faraday Trans*. *1* **86**, 271 (1990); (b) K. Ozutsumi, Y. Abe, R. Takahashi, S. Ishiguro. *J. Phys. Chem.* **98**, 9894 (1994).
49. Y. Zhang, N. Watanabe, Y. Umebayashi, S. Ishiguro. *J. Mol. Liq.* **119**, 167 (2005).
50. K. Fujii, Y. Umebayashi, R. Kanzaki, D. Kobayashi, R. Matsuura, S. Ishiguro. *J. Solution Chem.* **34**, 739 (2005) and papers therein.
51. K. Fujii, T. Kumai, T. Takamuku, Y. Umebayashi, S. Ishiguro. *J. Phys. Chem. A* **110**, 1798 (2006).
52. Y. Umebayashi, K. Matsumoto, Y. Mune, Y. Zhang, S. Ishiguro. *Phys. Chem. Chem. Phys.* **5**, 2552 (2003).
53. Y. Umebayashi, B. Mroz, M. Asada, K. Fujii, K. Matsumoto, Y. Mune, M. Probst, S. Ishiguro. *J. Phys. Chem. A* **109**, 4862 (2005).
54. V. Gutmann. *The Donor and Acceptor Approach to Molecular Interactions*, Plenum Press, New York (1978).
55. Y. Marcus. *The Properties of Solvents*, John Wiley, Chichester (1998).
56. Y. Umebayashi, T. Sukizaki, K. Fujii, S. Ishiguro. To be published.
57. Y. Umebayashi, T. Fujimori, T. Sukizaki, M. Asada, K. Fujii, R. Kanzaki, S. Ishiguro. *J. Phys. Chem*. *A* **109**, 8976 (2005).
58. K. Fujii, T. Fujimori, T. Takamuku, R. Kanzaki, Y. Umebayashi, S. Ishiguro. *J. Phys. Chem. B Lett.* **110**, 8179 (2006).
59. Y. Umebayashi, Y. Mune, T. Tsukamoto, Y. Zhang, S. Ishiguro. *J. Mol. Liq.* **119**, 177 (2005).
60. Y. Zhang, N. Watanabe, Y. Miyawaki, Y. Mune, K. Fujii, Y. Umebayashi, S. Ishiguro. *J. Solution Chem.* **34**, 739 (2005).
61. T. Ogura, Y. Murakami, Y. Ishimaru, S. Hayami, Y. Umebayashi, S. Ishiguro. To be published.